Supplement of Atmos. Chem. Phys., 21, 2067–2082, 2021
https://doi.org/10.5194/acp-21-2067-2021-supplement

Atmospheric Chemistry and Physics
Open Access

Supplement of

High-resolution hybrid inversion of IASI ammonia columns to constrain US ammonia emissions using the CMAQ adjoint model

Yilin Chen et al.

Correspondence to: Armistead G. Russell (ar70@ce.gatech.edu)

List of Figures

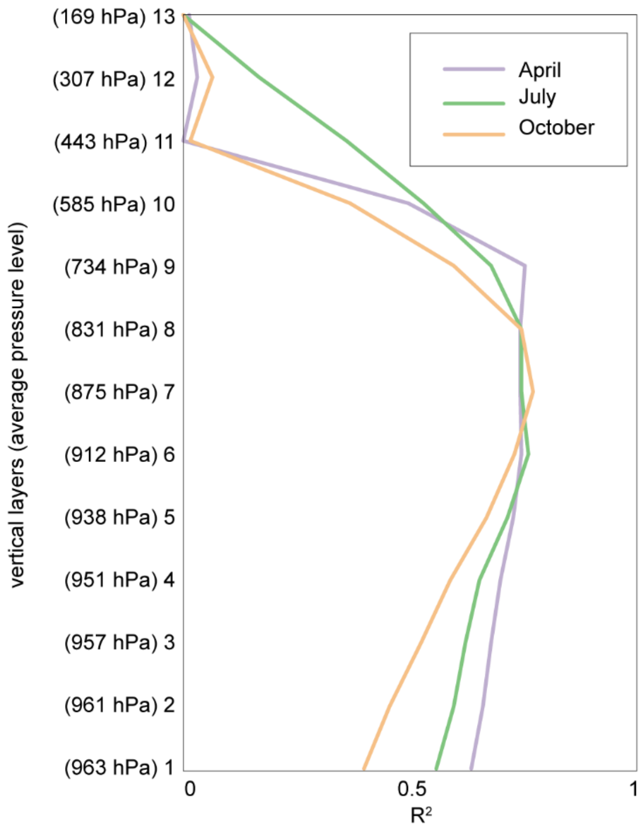

Figure S1 The correlation between monthly average CMAQ simulated NH_3 column densities and NH_3 concentrations at all 13 layers in April, July, and October. The grid cells with satellite observations are sampled at the IASI overpassing time. Monthly average NH_3 column densities and concentrations are calculated for each grid cell. R^2 for all data pairs in each month are calculated.

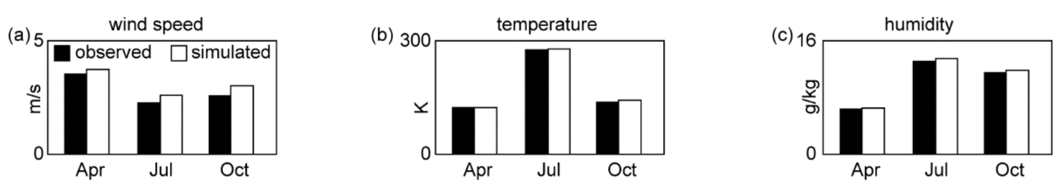

	Apr	Jul	Oct
Bias (m/s)	0.24	0.40	0.55
RMSE (m/s)	2.09	1.86	1.90

	Apr	Jul	Oct
Bias (K)	0.02	0.19	0.34
RMSE (K)	2.22	2.04	2.09

	Apr	Jul	Oct
Bias (g/kg)	0.11	0.41	0.20
RMSE (g/kg)	1.19	1.88	1.13

Figure S2 Model evaluation for WRF simulated meteorological fields against TDL hourly observations for April, July, and October. The bias and RMSE are listed below each plot.

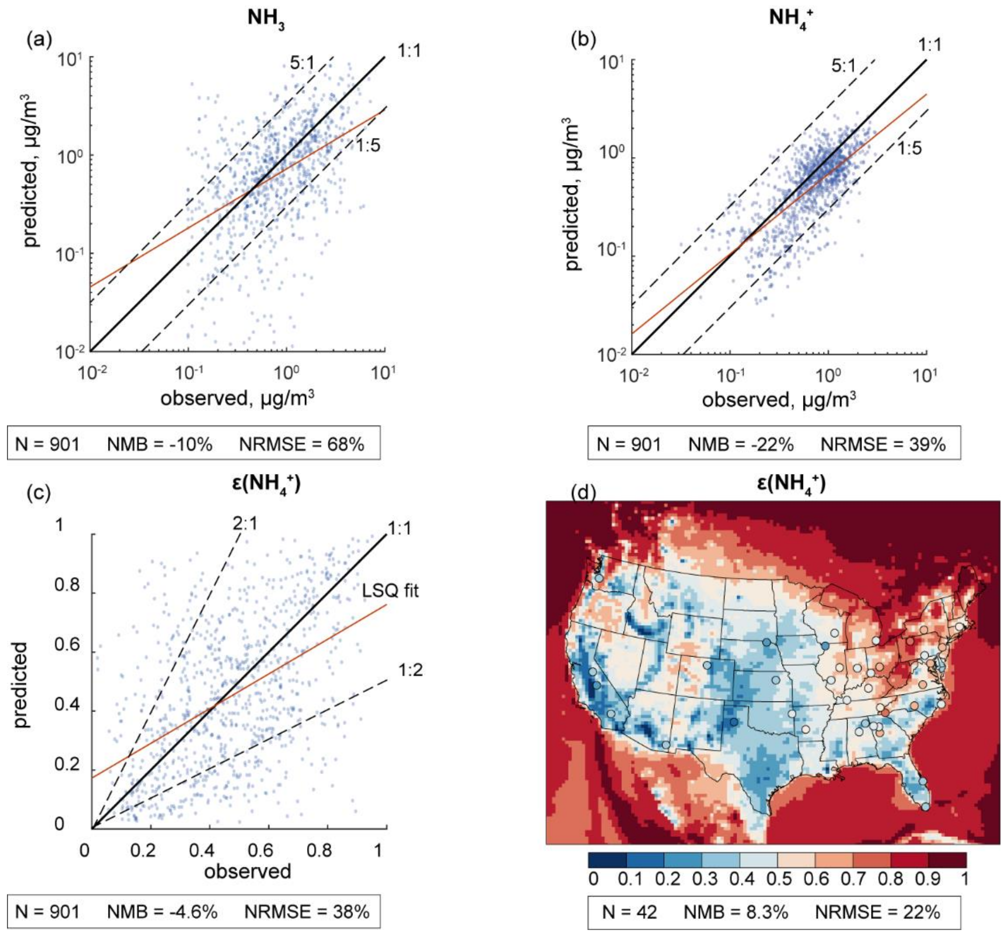

Figure S3 Model evaluation for CMAQ simulated bi-weekly average surface concentrations of NH_3 (a), NH_4^+ (b), and the gas-particle partitioning ratios, $\varepsilon(NH_4^+)$ (c) against observations from collocated AMoN (Ammonia Monitoring Network) and CASTNET (Clean Air Status and Trends Network) sites. Overlay of annual mean $\varepsilon(NH_4^+)$ based on simulated (color map) and observed (colored dots) concentrations are also plotted (d). The 1:1 line (solid black line), data range line (dashed back line with ratio labeled) and regression line (red) is also plotted. Number of data points (N), NMB, and NRMSE are provided along each plot.

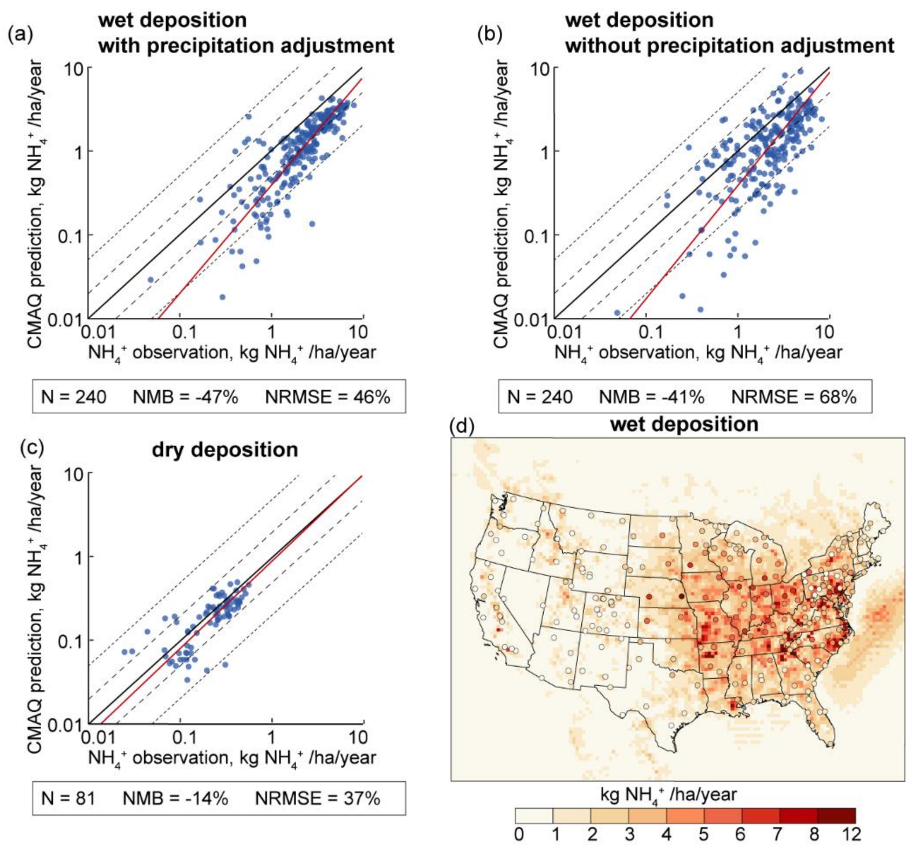

Figure S4 Model evaluation for CMAQ simulated wet (a and b) and dry (c) deposition of NH_4^+ against observations from the NADP (National Atmospheric Deposition Program) and the CASTNET (Clean Air Status and Trends) Network. Overlay of annual NH_4^+ wet deposition based on simulated (color map) and observed (colored dots) amount are also plotted (d). The scatter plots show the comparison between CMAQ predicted and observed annual dry, wet, and total deposition amounts, with the blue line showing the linear regression line. The 1:1 line (solid black line), data range line (dashed back line with ratio labeled) and regression line (red) is also plotted. Number of data points (N), NMB, and NRMSE are provided along each plot. For wet deposition, the CMAQ model performance with (a) and without (b) precipitation adjustment are evaluated.

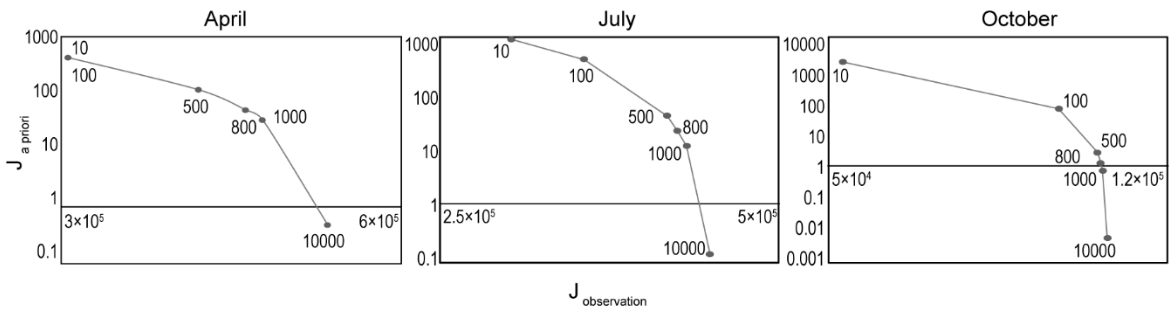

Figure S5 The L-curve for regularization factor (γ) value selection for April, July, and October. The error weighted squared difference between emission scaling factor and the a priori values ($J_{\textit{a priori}}$) is plotted against error weighted squared difference between IASI-NH_3 and simulated column density ($J_{observation}$) with different choices of γ values as denoted along the curve.

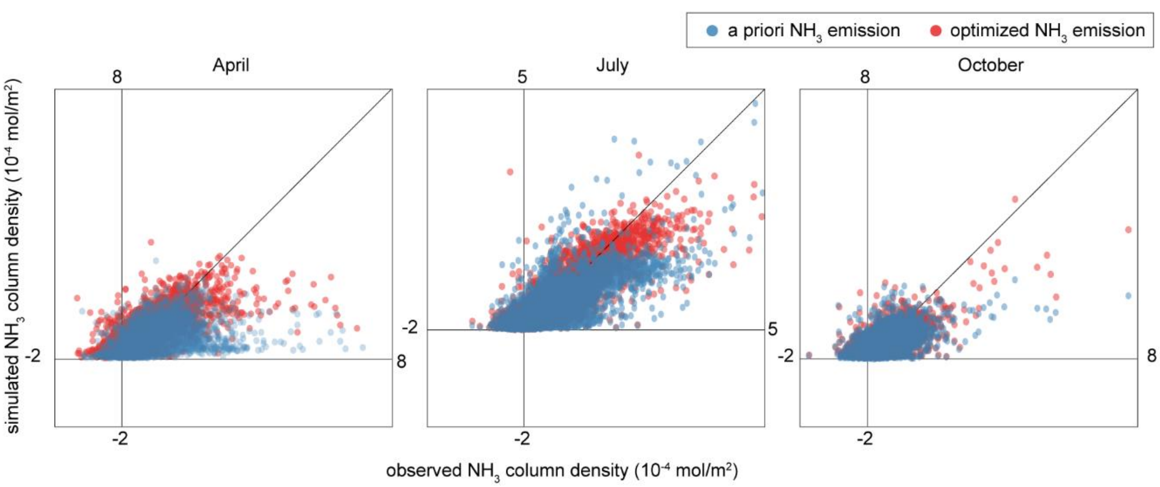

Figure S6 Comparison between simulated NH_3 column density against the IASI-NH_3 observations in April, July, and October using *a priori* (blue dots) and optimized NH_3 emission estimates (red dots).

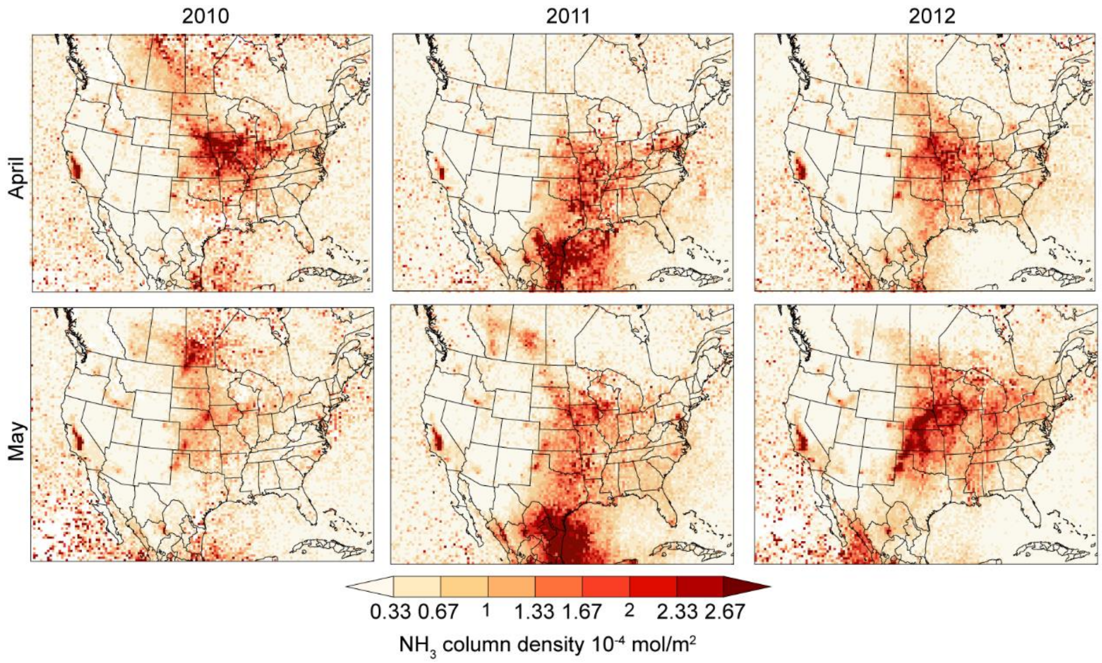

Figure S7 Monthly averaged IASI-NH_3 column densities in April and May from 2010 to 2012. The satellite retrievals are regridded at 36 km by 36 km resolution.

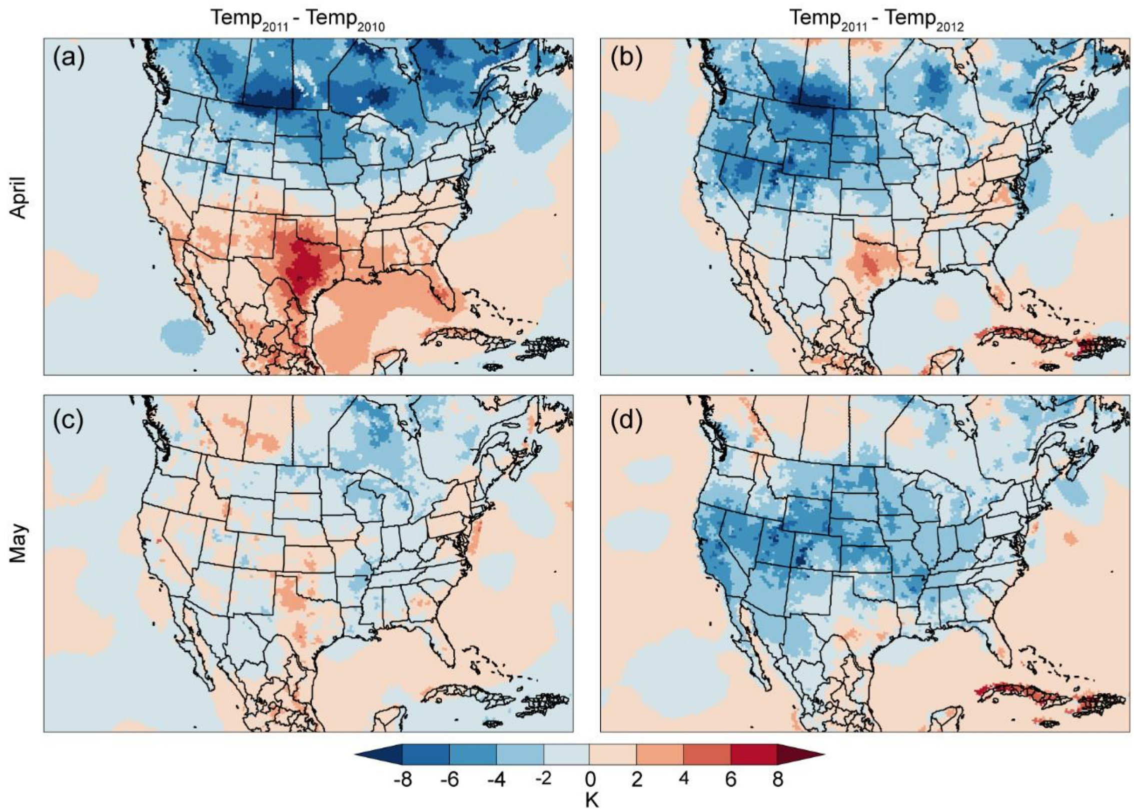

Figure S8 The monthly averaged surface temperature in April and May from 2010 to 2012.

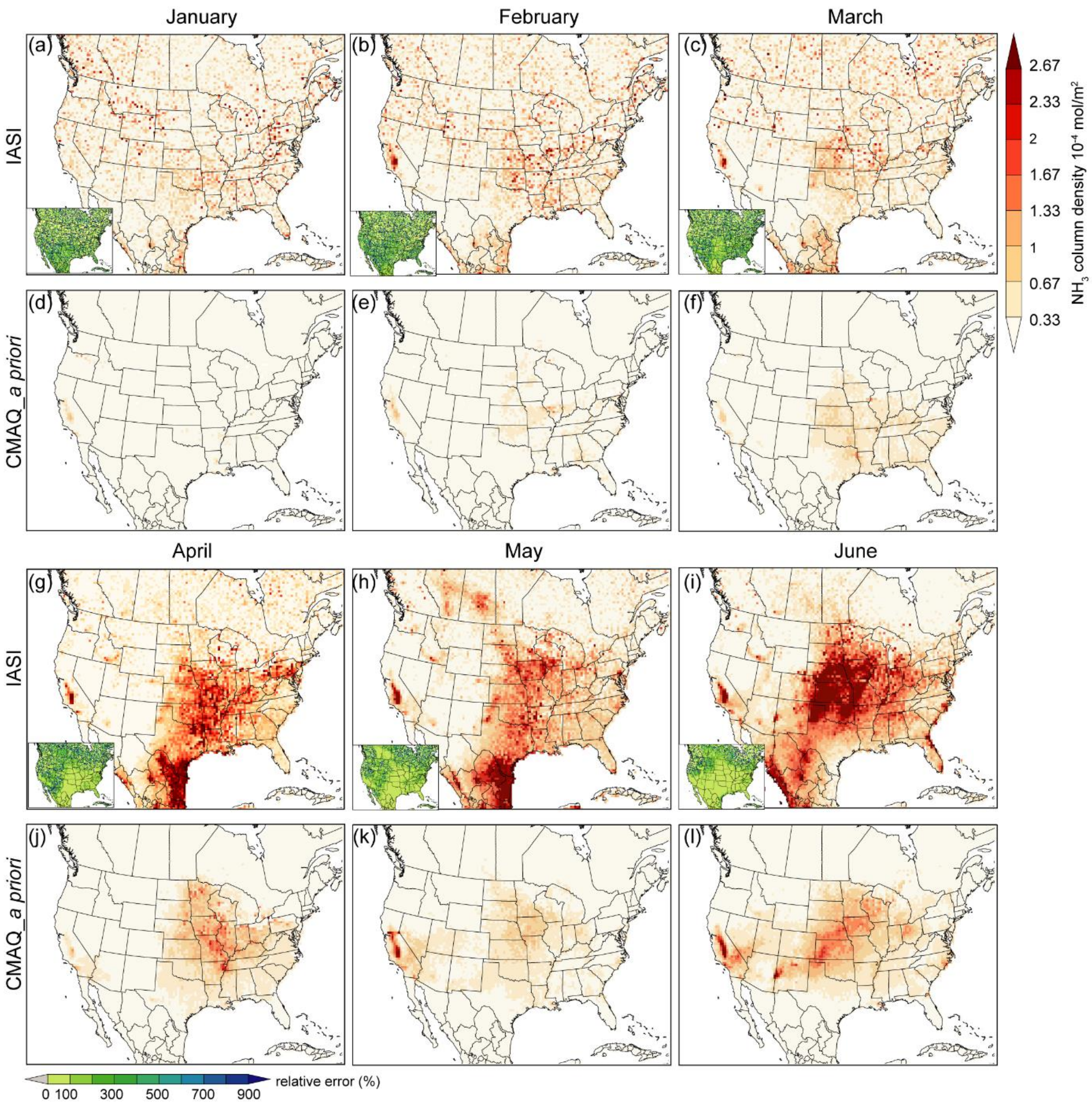

Figure S9 Comparison between monthly average IASI NH_3 column density (a-c, g-i, m-o, s-u) and CMAQ simulated values (d-f, j-l, p-r, v-x) based on the *a priori* NH_3 emission inventory in 2011. The monthly average relative error associated with the observed IASI NH_3 column density is shown in the corner of the corresponding plots.

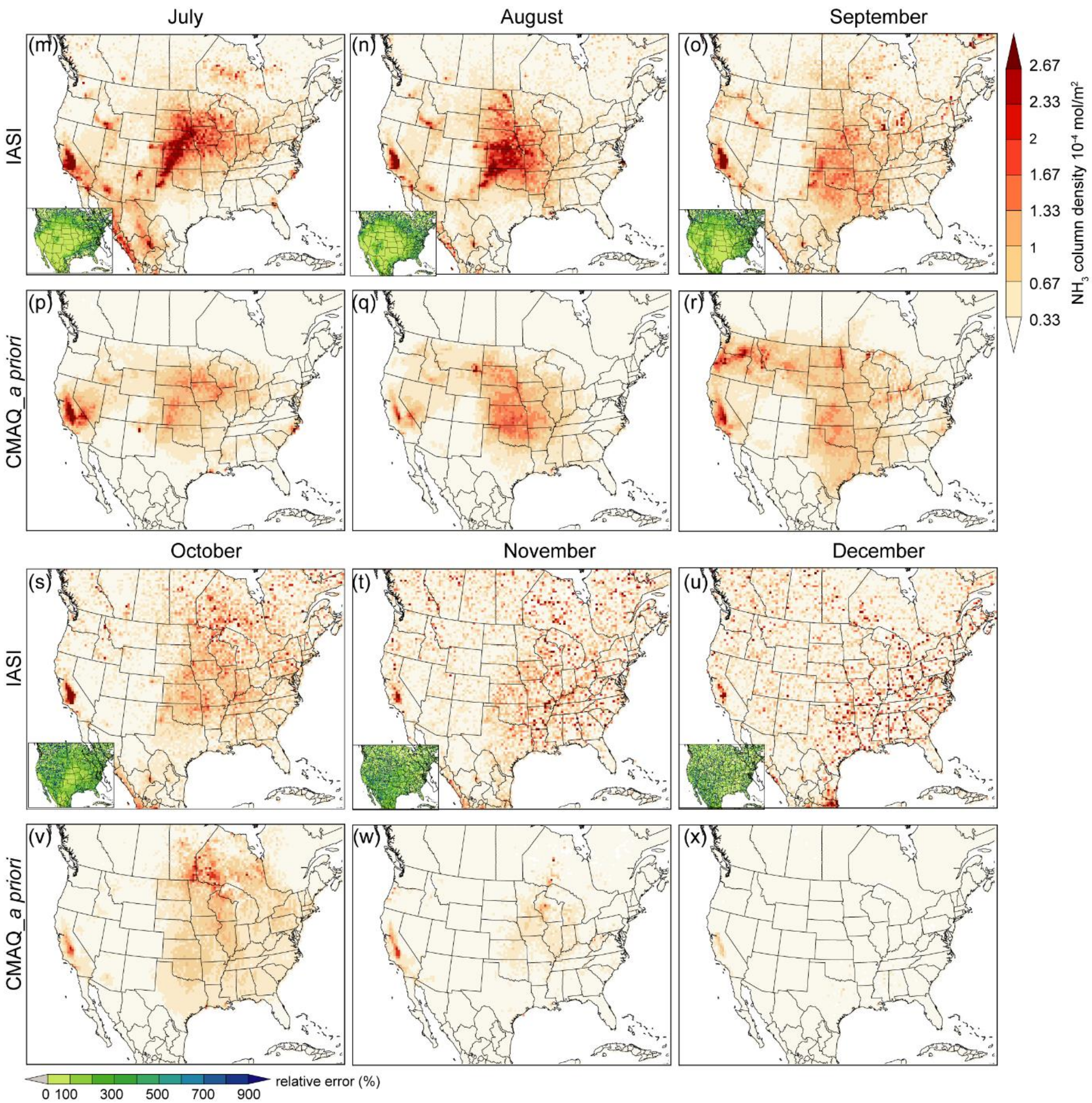

Figure S9 (continued) Comparison between monthly average IASI NH_3 column density (a-c, g-i, m-o, s-u) and CMAQ simulated values (d-f, j-l, p-r, v-x) based on the *a priori* NH_3 emission inventory in 2011. The monthly average relative error associated with the observed IASI NH_3 column density is shown in the corner of the corresponding plots.

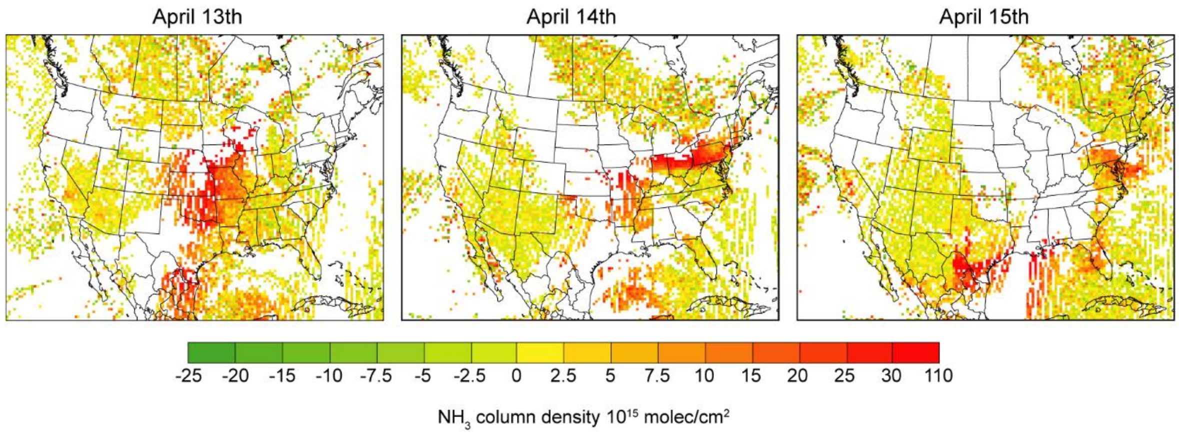

Figure S10 IASI NH_3 column density in April 13[th], 14[th], and 15[th] at 36 m by 36 km resolution within the model simulation domain of this study.

A trajectory analysis was performed using NOAA HYSPLIT model driven by meteorological fields forecasted by the North American Mesoscale Forecast System (NAM) at 12 km by 12 km resolution. Forward trajectory simulation was performed for April 13th to 15th with a source located in Oklahoma at surface level (37.0 N, 94.7 W). Backward trajectory simulation was performed for April 15th with a receptor located in Pennsylvania (40.9 N, 77.6 W) at both surface level and elevated level (5 km). The forward air parcel trajectories show that long-range transport toward northern and northeastern regions occurred on April 14th and 15th. The backward air parcel trajectories also show that NH_3 in elevated height may came in from the central U.S.

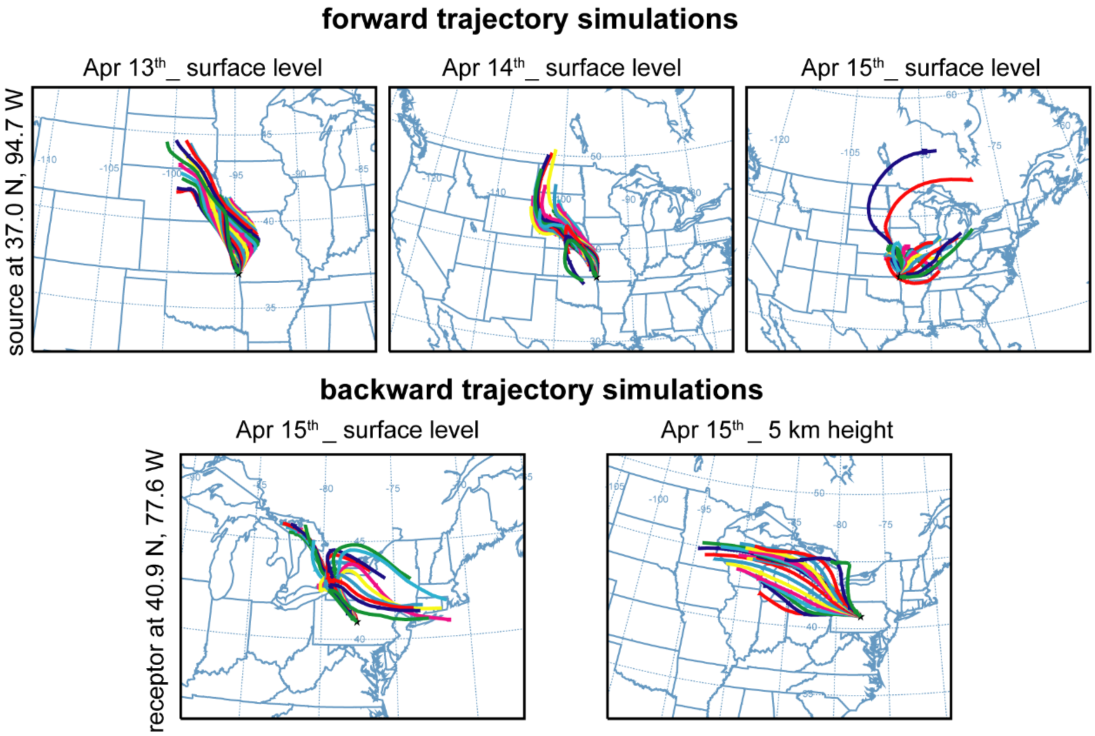

Figure S11 Forward and backward trajectory analysis generated from the NOAA HYSPLIT model. The location of the source (forward) and receptor (backward) are shown as stars in the figures. The starting time of each trajectory is 1 hour apart, from 00:00 to 24:00 local time on each day.

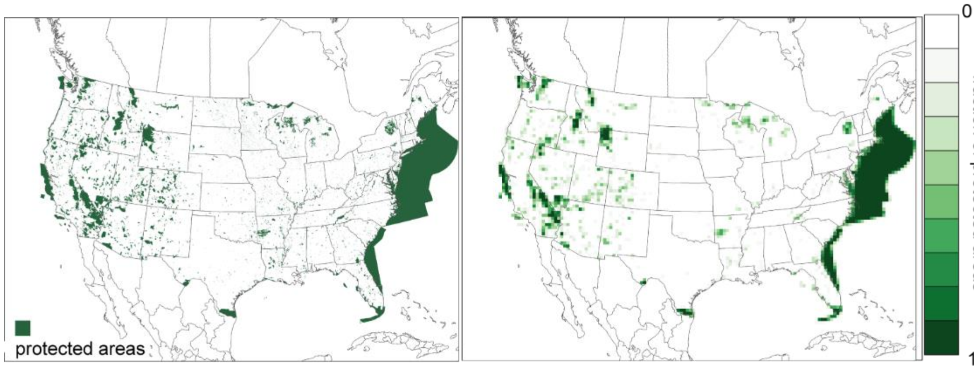

Figure S12 Protected areas for biodiversity conservation defined by the U.S. Geological Survey (USGS) Gap Analysis Project (A). And fraction of protected areas in each 36 km by 36 km simulated grids in this study (B).